01 Dec 1983

Charge Transfer And Ionisation Processes Involving Multiply Charged Ions In Collision With Atomic Hydrogen

D. J.W. Hardie

Ronald E. Olson
Missouri University of Science and Technology, olson@mst.edu

Recommended Citation

D. J. Hardie and R. E. Olson, "Charge Transfer And Ionisation Processes Involving Multiply Charged Ions In Collision With Atomic Hydrogen," *Journal of Physics B: Atomic and Molecular Physics*, vol. 16, no. 11, pp. 1983 - 1996, article no. 018, IOP Publishing, Dec 1983.
The definitive version is available at https://doi.org/10.1088/0022-3700/16/11/018

Charge transfer and ionisation processes involving multiply charged ions in collision with atomic hydrogen

J. Phys. B: At. Mol. Phys. **16** (1983) 1983–1996. Printed in Great Britain

Charge transfer and ionisation processes involving multiply charged ions in collision with atomic hydrogen

D J W Hardie and R E Olson

Department of Physics, University of Missouri-Rolla, Rolla, MO 65401, USA

Received 4 January 1983

Abstract. Total cross sections are presented for the charge transfer reaction

$$X^{q+} + H(1s) \rightarrow X^{(q-1)+} + H^+$$

and ionisation process

$$X^{q+} + H(1s) \rightarrow X^{q+} + H^+ + e^-.$$

Here X^{q+} is a fully or partially stripped ion. The collision energy range lies between 25–200 keV amu^{-1}. Cross sections are also given for charge transfer into particular ionic n states and n, l states for energies of 25 and 50 keV amu^{-1}, where $X^{q+} = H^+, He^{2+}, C^{6+}, O^{8+}$. The calculations were performed by the classical trajectory Monte Carlo method of Olson and Salop, modified to allow for a better representation of the H(1s) electronic radial distribution. Good agreement is seen with previous classical calculations and with quantum calculations performed by Ryufuku and Watanabe and others. Our results exhibit excellent accord (within 20%) with the measurements of Shah and Gilbody.

1. Introduction

Considerable interest in collision processes between a positive ion, X^{q+}, and atomic hydrogen, has been invigorated by research in controlled thermonuclear fusion plasmas. In particular, total cross sections for both ionisation and charge transfer are required. Recently, charge transfer reactions producing excited ions, $X^{*(q-1)+}$, have warranted study as these processes provide a means of impurity ion identification by subsequent detection of the characteristic radiation.

A wide range of collision energies (E, defined as keV amu^{-1}) exist in such plasmas. As a consequence, several theoretical descriptions are required, each pertaining to different dynamical regimes of the colliding particles. At very low collision energy, E, where the relative nuclear velocity is small compared with the mean orbital speed of the active electron, considerable success has been achieved by the perturbed stationary states (PSS) approximation and related methods. At very high energies, the Born series becomes reliable since only a few terms are significant.

The aforementioned methods become unwieldy at intermediate energies, however. Here it is prudent to adopt a purely classical description of the collision as proposed by Abrines and Percival (1966).

We present total cross sections for the ionisation

$$X^{q+} + H(1s) \rightarrow X^{q+} + H^+ + e^- \quad (1)$$

and charge transfer

$$X^{q+} + H(1s) \rightarrow X^{(q-1)+}(n, l) + H^+ \tag{2}$$

reactions (Q_I and Q_c respectively) in the collision energy range $25 \leqslant E \leqslant 200$ keV amu^{-1}. In (2) the final ionic state is specified by the principal and angular momentum quantum numbers $\{n, l\}$ with cross section, Q_c^{nl}. The total charge transfer cross section into all final states is $Q_c = \Sigma_n Q_c^n = \Sigma_{nl} Q_c^{nl}$, where Q_c^n is the cross section into a given n. Also presented are calculations of Q_c^n and Q_c^{nl} for $E = 25$ and 50 keV amu^{-1} with $X^{q+} = H^+$, He^{2+}, C^{6+}, O^{8+}.

Our results are compared with the previous classical calculations of Olson and Salop (1977) and Olson (1981), and with the classical theory of Eichenaur *et al* (1981) on proton–hydrogen collisions. Comparisons are made with the quantal calculations of Ryufuku and Watanabe (1979) and Ryufuku (1982) based on the unitarised distorted wave (UDW) approximation. This work is also contrasted with the PSS calculations, conducted on $C^{6+} + H$, of Green *et al* (1982) and with those of Chan and Eichler (1979), utilising the eikonal and Oppenheimer–Brinkman–Kramers methods (E-OBK), performed on protons in collision with atomic hydrogen. Our calculated total cross sections for ionisation Q_I, charge transfer Q_c, and electron loss $Q_L = Q_I + Q_c$, are discussed with reference to recent measurements by Shah and Gilbody (1981a, b).

In § 2, the theory of classical collisions and, in particular, a classical description of the target atom is given. The total ionisation, charge transfer and electron loss cross sections calculated here are presented and discussed in § 3. Section 4 deals with the partial charge transfer cross sections, Q_c^n and Q_c^{nl}, which are obtained for $X^{q+} = H^+$, He^{2+}, C^{6+}, O^{8+} and are compared with results of other workers. Summary and conclusions are given in § 5.

2. Theory

To describe, classically, a collision between a target atom (e.g. H) and a projectile ion, some attempt at a classical representation of the target atom is required. Many such one-electron classical atoms (CA) have been proposed (Percival and Richards 1975, Eichenaur *et al* 1981), the choice of which is crucial. Having adopted such a model, the three-body collision problem becomes a matter of simply solving Kepler's equation of planetary motion for the electron's orbit, and then integrating the twelve coupled Hamilton's equations for the motion. In our case, the integration (when required) was performed using the classical trajectory Monte Carlo (CTMC) method as described by Olson and Salop (1977). In essence, the three-body collision is solved exactly, the limits being set by the number of trajectories computed and is purely statistical in nature.

Since the description is purely classical, all the collision information is encompassed by the classical three-body Hamiltonian. Following this, the probability of any final configuration or state can be extracted from the Hamilton's equations, provided a meaningful classical description of that state is possible.

By far the most widely used CA is that first proposed by Abrines and Percival (1966), based upon the microcanonical distribution. Here all classical electronic degrees of freedom are assigned equal probability, the overall binding energy, $-U$,

being fixed ($U>0$). For this model, the electronic phase-space distribution is

$$\rho(\boldsymbol{r}, \boldsymbol{p}) = \delta(H(\boldsymbol{r}, \boldsymbol{p}) - U)/k. \tag{3}$$

Here $\boldsymbol{r}, \boldsymbol{p}$ are the electronic position and momentum vectors relative to the atomic nucleus, k is a normalisation constant and H is the atomic Hamiltonian, which for a hydrogenic atom (with effective core charge Ze) takes the form

$$H(\boldsymbol{r}, \boldsymbol{p}) = p^2/2m - Ze^2/r. \tag{4}$$

We may obtain the radial, $\rho(r, U)$, and momentum, $\rho(p, U)$, distributions by integrating (3) over all possible momenta and positions, respectively:

$$\rho(r, U) = (16/\pi R_0^3) r^2 (R_0/r - 1)^{1/2} \tag{5}$$

and

$$\rho(p, U) = (32/\pi P_0^3) p^2 (p^2/P_0^2 + 1)^{-4} \tag{6}$$

where $R_0 = Ze^2/U$ and $P_0^2 = 2\,mU$. The momentum distribution (6) is equivalent to that obtained from the momentum Schrödinger equation (Percival and Richards 1975). Consequently at very high collision energies, the collision is well described by a binary encounter (Percival and Richards 1975) between the incoming ion and the bound electron with the exact momentum distribution. It is this appealing property which accounts for the widespread use of the microcanonical CA. However, the radial distribution (5) is seen to have a cut-off at R_0, corresponding to highly eccentric orbits. This is at variance with the Schrödinger picture which allows the electron a finite probability of being outside the classically accessible region, $r>R_0$. Accordingly, weak collisions, where the projectile impact parameter, b, is large ($b>R_0$) are poorly described.

We propose a different distribution to that based upon the microcanonical ensemble: the binding energy, U, of the CA, is varied to allow the electronic radial distribution to extend beyond $R_0 = 2.0$ au. A similar idea was adopted by Eichenaur *et al* (1981) derived from the Wigner phase-space distribution. Here, however, we focus attention primarily on reproducing the radial 1s distribution, $\phi_{1s}(r)$, over a range $0 \leq r \leq R^*$, where R^* is a large distance. The radial function was obtained by requiring that a discrete set of microcanonical radial distributions, $\rho(r, U_j)$, reproduce the exact quantum radial wavefunction, $\phi_{1s}(r)$, over the chosen range. We ensure that $\phi_{1s}(r) \sim \rho(r)$ and

$$\rho(r) = \sum_j a_j \rho(r, U_j) \tag{7}$$

where a_j are real and positive amplitudes and $\Sigma_j a_j = 1$. The amplitude, a_j, may be regarded as the probability of encountering the target atom with a binding energy U_j (table 1). The amplitudes were obtained by a least-squares fitting procedure. In similar fashion, the new momentum distribution is

$$\rho(p) = \sum_j a_j \rho(p, U_j). \tag{8}$$

The value of R^* was chosen to ensure that most of the exact 1s radial distribution was accounted for. The parameter, R^*, was increased until the amplitudes were insensitive to small changes in R^*. This condition was satisfied when $R^* \sim 4.0$ au.

Table 1. U_j and α_j for eight discrete radial functions (see equation (5)).

U_j	α_j
∞	0.000
2.0000	0.0160
1.0000	0.0984
0.6667	0.1923
0.5000	0.2185
0.4000	0.1849
0.3333	0.1349
0.2857	0.0920
0.2500	0.0630

The new radial distribution is seen to be very close to the 1s radial function (figure 1). The slight deviations for $r<R^*$ are mainly due to the normalisation requirement and also a discrete rather than a continuous, set of fitting functions was used. More significant deviations are seen in the momentum distribution (figure 2), however, these are not greater than those obtained by the procedure of Eichenaur *et al* (1981). The new momentum distribution is similar in shape to the exact quantal momentum distribution and spans the complete momentum space, thus, justifying its use for the scattering calculations. The slight difference between the exact and the modified classical momentum distributions should not severely affect the high-energy limit of the total cross sections.

Our procedure, which attempts to reproduce the exact 1s radial function may be regarded as the 'radial limit'. This is in contrast to the approach of Percival and co-workers which, using the conventional microcanonical distribution, can be said to be the 'momentum limit'. The theory of Eichenaur *et al* (1981), which treats both the radial and momentum distributions equivalently should therefore produce results bounded by these limits.

In our method, any quantity, Q, which can be classically defined, may be obtained from the set of corresponding quantities, $Q(U_j)$, evaluated for different binding

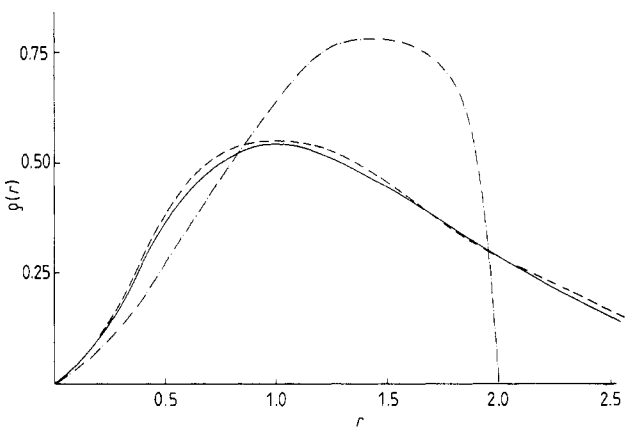

Figure 1. Radial distributions for H(1s): —•—; microcanonical; ——; quantum; – – –; this work.

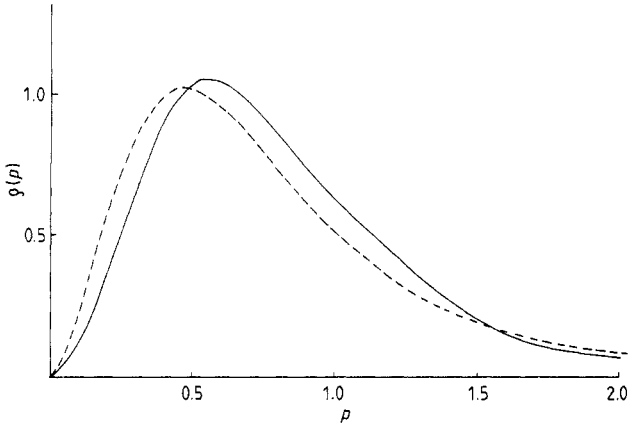

Figure 2. Momentum distributions for H(1s): ——; quantum/microcanonical; – – –; this work.

energies, U_j, using the CTMC and the microcanonical ensemble, hence

$$Q = \sum_j a_j Q(U_j). \tag{9}$$

Having thus found the amplitudes, a_j, the problem becomes that of simply calculating the relevant quantities (i.e. cross sections) for different target binding energies. The final statistical error in Q should be of similar order to the errors estimated for the $Q(U_j)$.

3. Total cross sections

In the particular case of the total cross sections for ionisation and charge transfer, it was convenient to make use of a simple scaling rule which arises from the symmetry of the classical collision Hamiltonian. This scaling allows the evaluation of the total cross section, Q, for a given process at any target binding energy, U, and collision energy, E, having previously determined Q at U_0 and E_0 respectively:

$$Q(E, U) = (U_0/U)^2 Q(E_0 U/U_0, U_0). \tag{10}$$

Using this property and (9) the total cross sections for ionisation Q_I, and charge transfer, Q_c, were calculated for processes (1) and (2) respectively.

Our procedure has the distinct advantage of being able to evaluate Q_I and Q_c from the original data of Olson and Salop (1977) and of Banks *et al* (1976) without the need to compute new trajectories.

Our calculated total ionisation cross section, Q_I, as a function of the collision energy E is shown (figure 3) for various charge states, q, of the fully stripped ion. The cross section, at low E, exhibits a sharp onset of the ionisation probability, in contrast to the gentler onset predicted by Olson and Salop (1977). The cross section maximum, $\tilde{Q}_I$ (for a given q) is also correspondingly larger than predicted by Olson and Salop (1977) and occurs at a lower collision energy, $\tilde{E}_I$. Typically our value of $\tilde{Q}_I$ exceeds the Olson and Salop (1977) prediction by 25–30% while our $\tilde{E}_I$ is lower by 5–30%. As far as overall behaviour is concerned, however, our Q_I has a similar

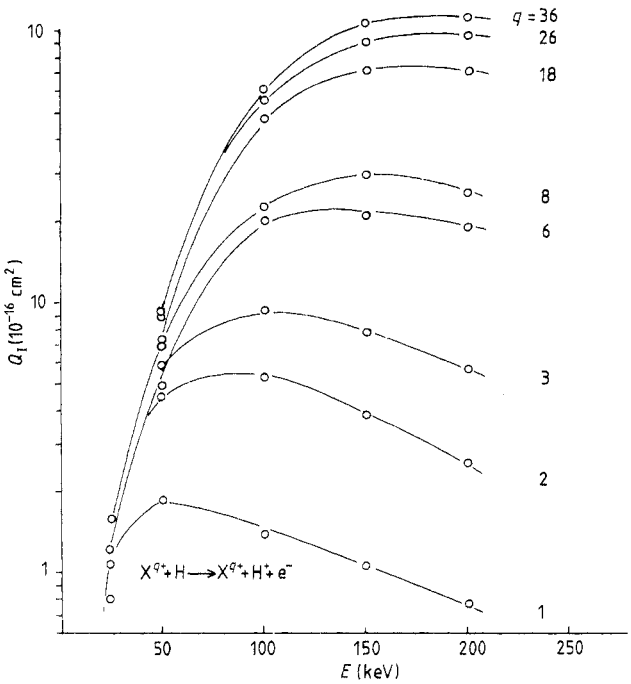

Figure 3. Total cross section for ionisation, Q_I (in 10^{-16} cm^2) where X^{q+} is a fully stripped ion.

energy dependence to that found by Olson and Salop (1977). At the highest E, both Q_I curves behave as $1/E$ and differ only by a constant factor, which from the binary encounter approximation, depends solely on the target binding energy, U (Percival and Richards 1975).

The sharper rise of our ionisation cross section and our larger $\tilde{Q}_I$ when compared to the Olson and Salop (1977) cross section may be easily attributed to the larger physical size of our CA and the finite probability of encountering a 'loosely bound' electron with binding energy, $U < \frac{1}{2}$ au.

The total cross section for charge transfer, Q_c, against collision energy is also shown (figure 4). Again a similar set of curves (pertaining to each q) to that of Olson and Salop (1977) was found. As in the case of ionisation, our predicted maximum, $\tilde{Q}_c$, is larger, by 20–40%, than the Olson and Salop (1977) value. Our $\tilde{Q}_c$ occurs at a lower collision energy, $\tilde{E}_c$, typically by 10–40%. At collision energies exceeding $\tilde{E}_c$, there is a faster fall-off in Q_c than obtained by Olson and Salop (1977). Due to the rapid rise in ionisation, a correspondingly faster decrease in the charge transfer probability ensues. On comparing our results with the UDW calculations of Ryufuku (1982), fair agreement is seen. In particular, our values of Q_c, for $X^{q+} = H^+$, Li^{3+}, C^{6+} are within 20% of the UDW cross section. For the case of ionisation, however, larger differences exist, our results generally being larger by up to 100%. This may be due to incompleteness of the basis functions used by Ryufuku (1982) to describe the continuum.

Cross sections for ionisation and charge transfer were also calculated for partially stripped ions. The ionic core is represented by an effective bare charge as discussed

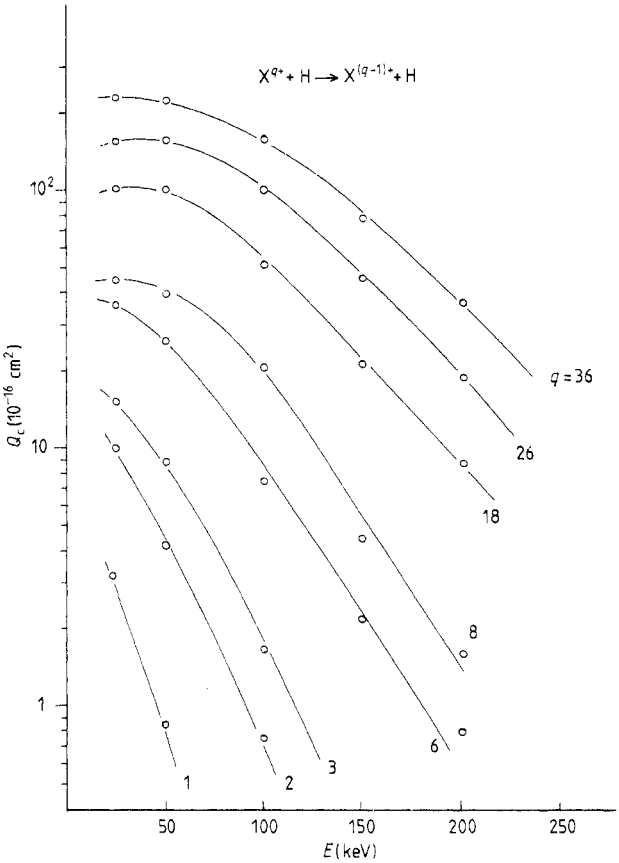

Figure 4. Total cross section for charge transfer, Q_c (in 10^{-16} cm^2) where X^{q+} is a fully stripped ion.

by Olson and Salop (1977). These calculations were performed on $A^{q+} = C^{q+}$, N^{q+}, O^{q+} $(2 < q < 5)$ and are directly comparable to the experiment of Shah and Gilbody (1981b) conducted on the ionisation process (2) and on the charge transfer reaction (1), the latter for the case of $X^{q+} = C^{3+}$, C^{4+}. Here again good accord is seen. In particular the plot of log Q_I against log q at fixed collision energy (~150 keV amu^{-1}) by Shah and Gilbody (1981b) is well reproduced by our results (figure 5). Our larger ionisation cross section maxima (compared with Olson and Salop 1977) qualitatively agrees with experiment (Shah and Gilbody 1981b) as well as with the lower collision energy at which the maxima occur.

Our calculated total electron loss cross section, $Q_L = Q_I + Q_c$, is very similar to the corresponding Olson and Salop (1977) calculation (figure 6). However, for each q value, our calculated Q_L exceeds that of Olson and Salop (1977) by up to about 40%, a manifestation of the larger physical size of our CA. In a similar manner to that of Olson *et al* (1978) we obtain the universal scaling curve (figure 6):

$$Q_L/q = 6.4 \times 10^{-16}\{23q/E[1-\exp(-E/23q)]\}\ \text{cm}^2 \tag{11}$$

where E is expressed in keV amu^{-1}. Here again our predictions are in good agreement

with the measurements of Shah and Gilbody (1981a, b) (figure 6). However, at these energies, ionisation dominates the electron-loss cross section so the above accord cannot be taken as a severe test of our charge-transfer cross section calculations.

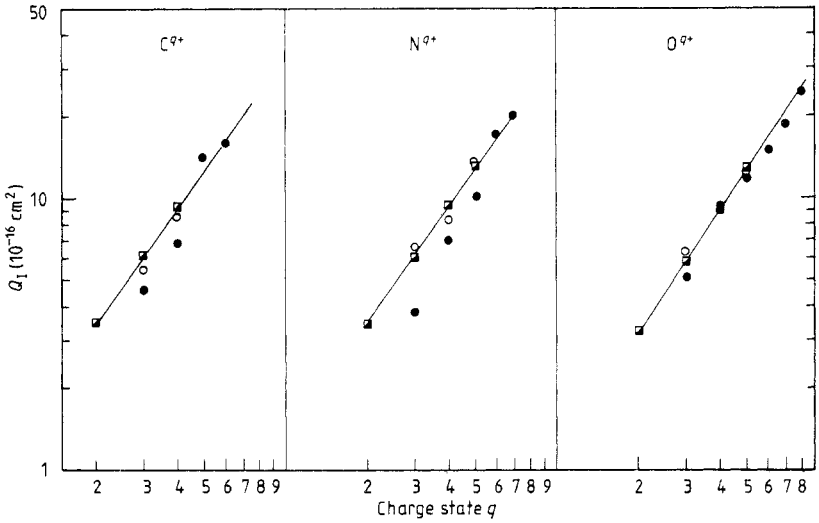

Figure 5. Plot of ionisation cross section, Q_I (in 10^{-16} cm^2), against ion charge state, q(X = C, N, O) for $E \approx 150$ keV amu^{-1}. ◪: Experiment (Shah and Gilbody 1981b); ●: Olson and Salop (1977); ○; This work.

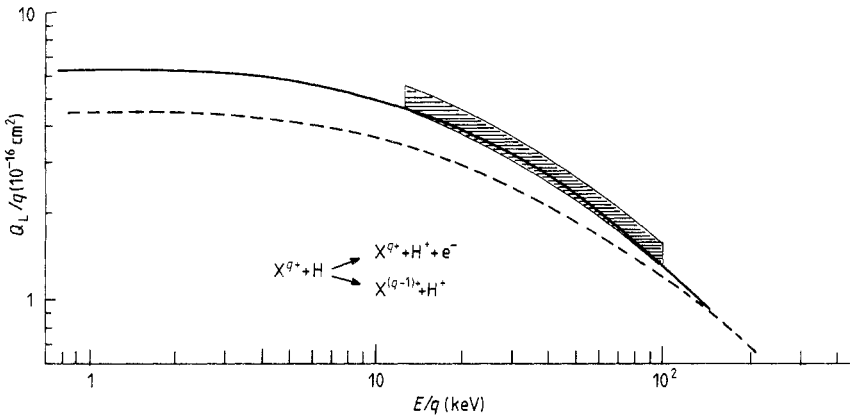

Figure 6. Plot of Q_L/q, where Q_L is the total electron loss cross section (in 10^{-16} cm^2) against E/q (keV/amu), where X is a fully or partially stripped ion. ---: Olson *et al* (1978); ——: this work; hatched area: Shah and Gilbody (1981a, b).

4. Charge transfer to particular final states

In addition to the total cross section for charge transfer into all final states, Q_c, the cross section, Q_c^{nl}, yielding a particular state with quantum numbers $\{n, l\}$ respectively was also evaluated for the reaction (2) with X^{q+} being a fully stripped ion. Here, however, no convenient scaling law exists for the Q_c^{nl} and new sets of trajectories had

to be computed for several different target binding energies, U. The cross section, Q_c^{nl}, was obtained in a similar manner to that of the total cross sections using (9).

The final-state quantum numbers $\{n, l\}$ cannot strictly be defined classically. However, the evaluation of the final classical electronic momentum relative to the projectile nucleus allows the final binding energy, U_f, and angular momentum, to be easily obtained. From these quantities, $\{n, l\}$ may be assigned using simple classical correspondence principles (Olson 1981). The final principal quantum number n, is thus given by

$$n = qe^2/(2U_f)^{1/2} \tag{12}$$

while the angular momentum quantum number is

$$l = [(x\dot{y} - y\dot{x}) + (x\dot{z} - z\dot{x}) + (y\dot{z} - z\dot{y})]^{1/2} \tag{13}$$

where x, y, z are the cartesian co-ordinates of the electron relative to X^{q+} and $\dot{x}$ denotes the corresponding velocity along $\hat{x}$. From (12) and (13), $\{n, l\}$ can be assigned from their continuous classical analogues by a suitable sampling technique. A detailed discussion of this procedure is given by Olson (1981).

The cross section Q_c^{nl} for reaction (2) was obtained for collision energies, $E = 25$ and 50 keV amu^{-1}. We shall first discuss the charge transfer cross section into a specific n, summing over all possible values of l, $Q_c^n = \Sigma_l Q_c^{nl}$.

4.1. Q_c^n

Our results for Q_c^n are displayed (figure 7) at collision energies of 25 and 50 keV amu^{-1} and for the charge states of interest here ($q = 1, 2, 6, 8$). Also shown are the corresponding calculations of Olson (1981) and for the particular case of $C^{6+}+H$ at $E = 25$ keV amu^{-1}, the UDW and PSS calculations of Ryufuku and Watanabe (1979) and Green *et al* (1982) respectively.

Reasonable accord is seen with the results of Olson (1981). The n distributions are seen to broaden with increasing E and q (figure 7). However our distributions are generally broader than the corresponding Olson (1981) distributions. Both sets of results are in agreement for the value of n, $\tilde{n}$, where the maximum cross section, $\tilde{Q}_c^n$, occurs and are virtually indistinguishable for $n \leqslant \tilde{n}$. The disparity at large $n > \tilde{n}$ may be attributed to two factors. Firstly for a given set of initial conditions there is a tendency for the active electron to conserve its initial quantum numbers and dynamical configuration (Olson 1981). Since our CA breathes by varying its binding energy, this in effect brings about a subsequent broadening in the initial quantum numbers (primarily n). This therefore gives rise to a slight smearing of final quantum numbers $\{n, l\}$. Secondly, the possibility of larger initial Kepler orbits in our model, in contrast to that of Olson (1981), increases the probability of capture at large impact parameters. This in turn produces final orbits which tend to be physically larger than obtained by Olson (1981), with correspondingly higher $\{n, l\}$.

The broader behaviour of our n distributions (for a given collision energy), compared with the results of Olson (1981) is in qualitative agreement with the quantal calculations of Ryufuku and Watanabe (1978) and of Green *et al* (1982), performed on $C^{6+}+H$. Our results are consistent with the above authors, in the value of $\tilde{n}$ being less than q, the projectile charge state. We also confirm the prediction of Olson (1981), namely $\tilde{n} = n_i(q/q_i)^{3/4}$, where n_i, q_i are the initial principal quantum number and target nuclear charge state respectively.

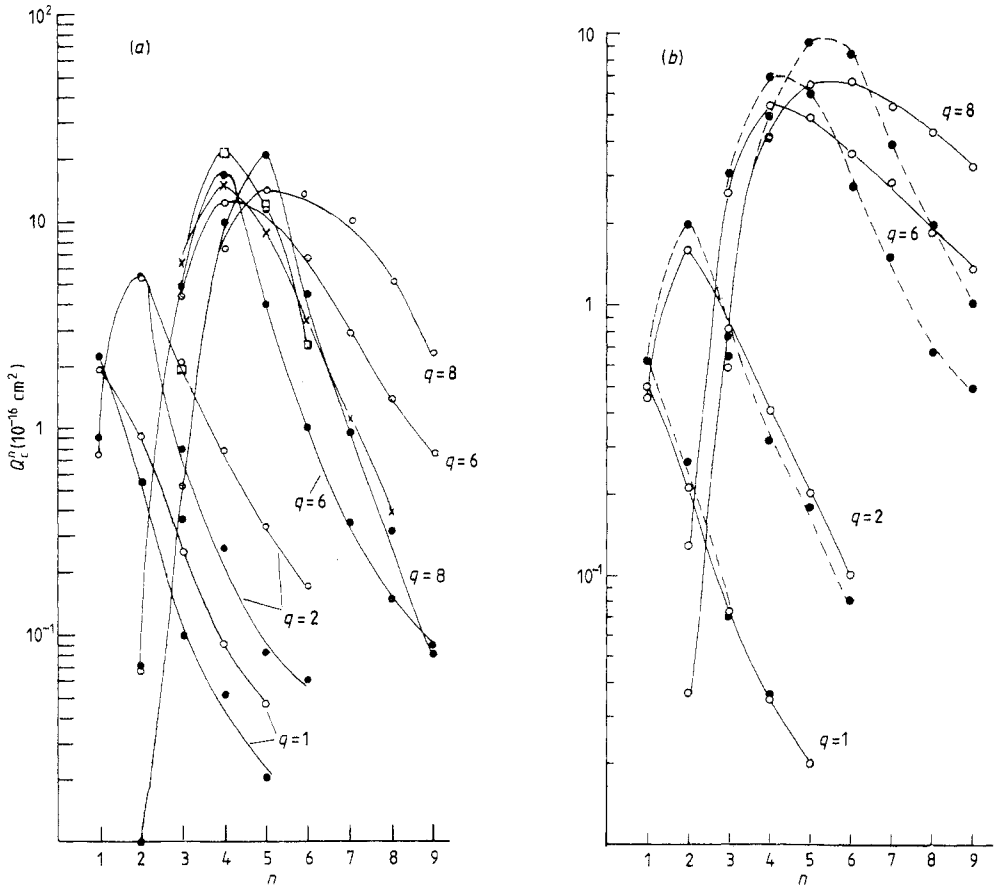

Figure 7. Charge transfer cross section, Q_c^n (in 10^{-16} cm^2), into a particular n level. (*a*) $E = 25$ keV amu^{-1}, □: Green *et al* (1982) for $q = 6$; ×: Ryufuku and Watanabe (1979) for $q = 6$; $E = 50$ keV amu^{-1}, ●: Olson (1981); ○: this work. (*b*) $E = 50$ keV amu^{-1}, ●: Olson (1981); ○: this work.

4.2. Q_c^{nl}

The charge transfer cross section yielding a particular final electronic state $\{n, l\}$, Q_c^{nl} are also shown (figure 8) for the reactions considered above ($n \leq 6$). Again our results are similar to those obtained by Olson (1981), although they are slightly broadened. At $E = 50$ keV amu^{-1}, there is excellent accord (figure 8) with Olson (1981) for all $\{n, l\}$ $n < \tilde{n}$: here both sets of results predict a large bias towards the largest possible values of l ($l = n - 1$). For values of n larger than the preferred maximum, $\tilde{n}$, the most preferred value of l, $\tilde{l}$, indicated by this work is also that found by Olson (1981). In consequence our results find little deviation from the observed result of Olson (1981), namely $\tilde{l} = \tilde{n}$. Only at larger values of l, above $\tilde{l}$, are there marked differences between this work and Olson (1981) and these decrease slightly with increasing projectile charge state, q. Our large value of Q_c^{nl} for $n > \tilde{n}$, $l > \tilde{l}$ can be attributed to the smearing of the Kepler orbits in our CA. This extends the possible range of orbit eccentricities which may yield capture (for large impact parameter) in contrast to the rather narrow band of eccentric orbits (low l) allowed by the microcanonical CA of Olson (1981).

On comparing this work with eikonal calculations of Chan and Eichler (1979) for $H^+ + H$ collisions (figure 8(*e*)), a marked disparity is seen as far as overall trend is concerned. The reasons for this are unclear; however, both sets of calculations are similar in magnitude.

Our results at low $E(=25\,\text{keV amu}^{-1})$ again exhibit similar trends to those presented by Olson (1981) (figure 8(*a*)–(*d*)). In addition, our calculations of Q_c^{nl}, performed on $C^{6+} + H$ may be directly compared with the UDW calculations of Ryufuku and Watanabe (1979) and the PSS theory of Green *et al* (1982). Here good qualitative agreement is found for $\{n, l\} < \{\tilde{n}, \tilde{l}\}$ with our predicted values being well within 50% of the quantal results. It must be stressed, however, that at this low

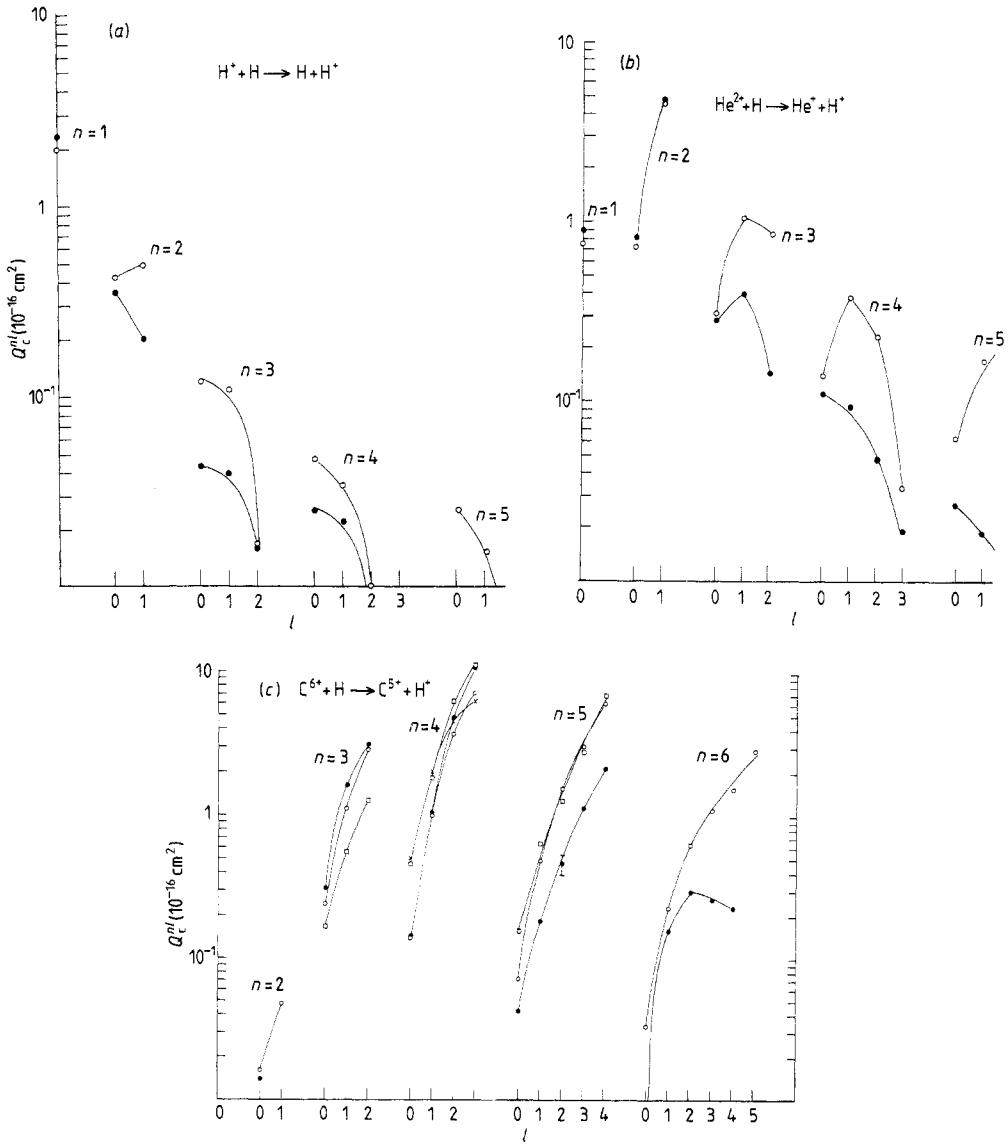

Figure 8.

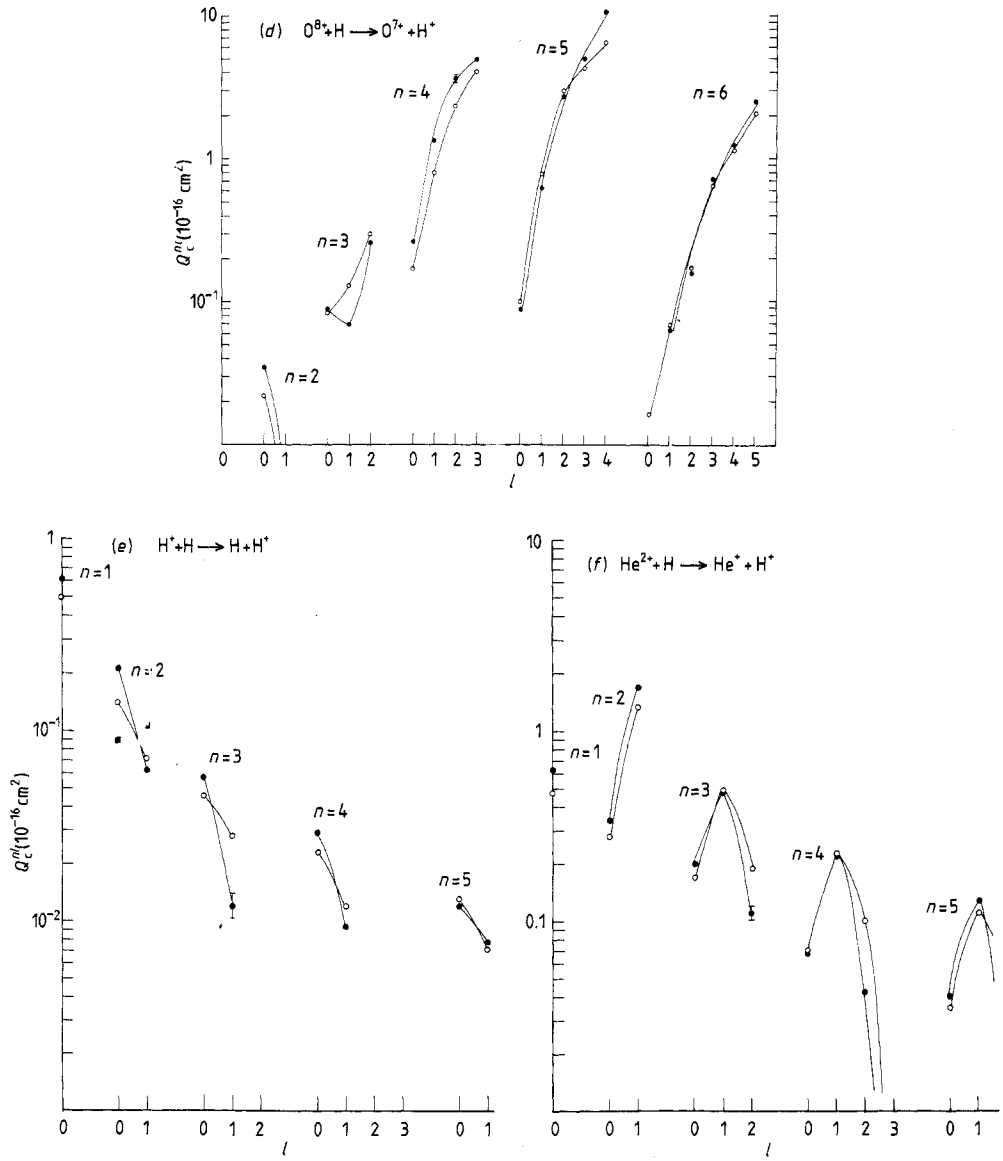

Figure 8.

energy, the classical dynamical description may be unreliable and our results are quoted simply for completeness. The unreliability is manifest here since the electronic motion is more in keeping with a molecular 'cloud' rather than a classical Kepler orbit.

5. Summary and conclusion

Calculations of the cross sections for ionisation and charge transfer processes between a multiply charged ion and atomic hydrogen were performed for collision energies

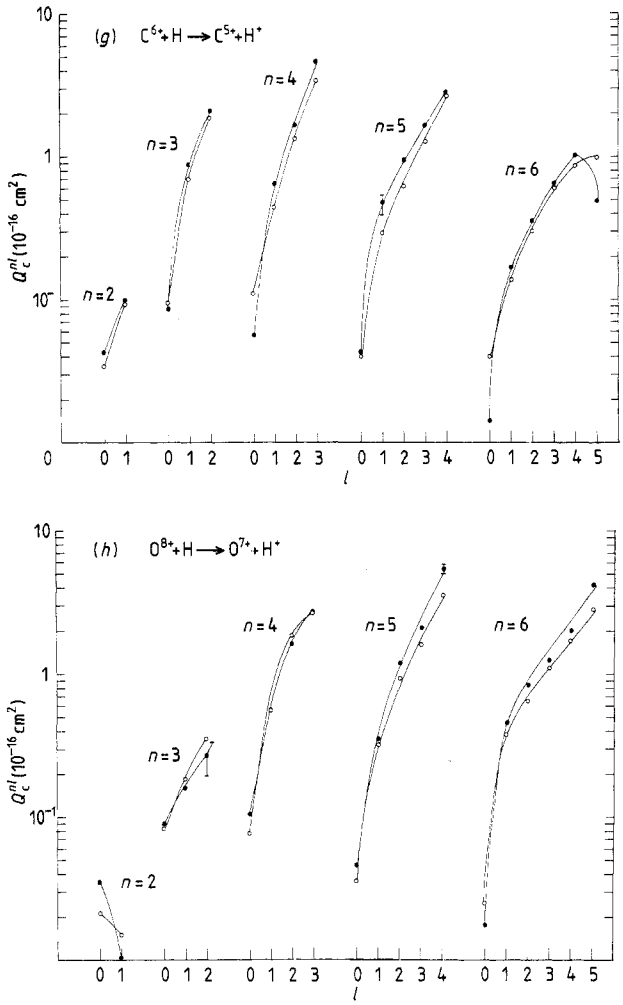

Figure 8. Charge transfer cross section, Q_c^{nl} (in 10^{-16} cm^2), into a particular $\{n, l\}$ level. Indicated by error bars are typical uncertainty estimates (one standard deviation, shown when large enough). (*a*)–(*d*) $E = 25$ keV amu^{-1}, □: Green *et al* (1982) for $q = 6$; ×: Ryufuku and Watanabe (1979) for $q = 6$; ●: Olson (1981); ○: this work. (*e*)–(*h*) $E =$ 50 keV amu^{-1}; ●: Olson (1981); ○: this work; ■: Chan and Eichler (1979) for $q = 1$.

25–200 keV amu^{-1}. The collision was described classically, the integrations were carried out by the CTMC method.

It was thought timely by the authors to endeavour to improve on the target atom electronic radial distribution by attempting to incorporate some quantal effects. The results of this work could be compared with previous work based upon the classical microcanonical atomic model (Olson and Salop 1977, Olson 1981), which may be deemed the momentum limit. Thus it was possible to extract two bounds to the CTMC procedure: the 'momentum' and 'radial' limits.

Improving the radial distribution generally produces an increase in the ionisation probability and yields better accord with recent measurements (Shah and Gilbody 1981a, b). The charge transfer cross section is fairly insensitive as to which limit is

adopted particularly at energies above 25 keV amu^{-1}. The basic predictions and scalings found by Olson (1981) are seen to be unchanged in the radial limit.

The disadvantages of adopting the radial limit are obvious. Clearly the classical momentum distribution no longer reproduces the exact quantum result. However, we claim that the overall shape of the momentum distribution is not severely transformed in going to the radial limit. The momentum distribution retains its overall character and limits for $p \to \infty, p \to 0$. Accordingly averaging over all possible binding energies should not produce frequent trajectories with an unphysical initial electronic momenta. It may also be added that only at very high collision energies is the binary encounter limit valid, which is crucially dependent on the momentum distribution (Percival and Richards 1975). At these high energies, however, quantum effects dominate (e.g. tunnelling).

It may be seen that in general, the CTMC procedure yielded similar predictions in the two limits, indicating that the actual collision dynamics are well described classically. We may conclude, therefore, that this lends further credence to the CTMC method as being a reliable means of calculating cross sections in this dynamical regime. It is hoped that the success of the purely classical description of the collision dynamics, for these collision energies, may stimulate further work in incorporating semi-classical techniques to these problems.

Acknowledgments

This work is supported by a grant from the Magnetic Fusion Division, US Department of Energy.

References

Abrines R and Percival I C 1966 *Proc. Phys. Soc.* **88** 873–83
Banks D, Barnes K S and Wilson J McB 1976 *J. Phys. B: At. Mol. Phys.* **9** L141–4
Chan F T and Eichler J 1979 *Phys. Rev.* A **20** 1841–7
Eichenaur D, Grün N and Scheid W 1981 *J. Phys. B: At. Mol. Phys.* **14** 3929–41
Green T A, Shipsey E J and Browne J C 1982 *Phys. Rev.* A **25** 1364–73
Olson R E 1981 *Phys. Rev.* A **24** 1726–33
Olson R E, Berkner K H, Graham W G, Pyle R V, Schlacter A S and Stearns J W 1978 *Phys. Rev. Lett.* **41** 163–6
Olson R E and Salop A 1977 *Phys. Rev.* A **16** 531–41
Percival I C and Richards D 1975 *Adv. At. Mol. Phys.* **11** 1–82
Ryufuku R 1982 *Phys. Rev.* A **25** 720–35
Ryufuku R and Watanabe T 1979 *Phys. Rev.* A **20** 1828–37
Shah M B and Gilbody H B 1981a *J. Phys. B: At. Mol. Phys.* **14** 2361–77
—— 1981b *J. Phys. B: At. Mol. Phys.* **14** 2831–41